Heat and Mass Transfer of a Non-Newtonian Fluid Flow over a Permeable Wedge in Porous Media with Variable Wall Temperature and Concentration and Heat Source or Sink

ALI J. CHAMKHA
Manufacturing Engineering Department
The Public Authority for Applied Education and Training
P. O. Box 42325
Shuweikh, 70654 – KUWAIT
E-mail: chamkha@paaet.edu.kw

Abstract: - The problem of steady, laminar, coupled heat and mass transfer by mixed convective flow of a non-Newtonian power-law fluid over a permeable wedge embedded in a porous medium with variable surface temperature and concentration and heat generation or absorption and wall transpiration effects is considered. A mixed convection parameter for the entire range of free-forced-mixed convection is employed and a set of non-similar equations are obtained. These equations are solved numerically by an efficient implicit, iterative, finite-difference method. The obtained results are checked against previously published work for special cases of the problem and are found to be in good agreement. A parametric study illustrating the influence of the various physical parameters on temperature and concentration profiles as well as the local Nusselt and Sherwood numbers is conducted. The obtained results are illustrated graphically and the physical aspects of the problem are discussed.

Key-Words: - Mixed convection, porous media, heat and mass transfer, heat generation/absorption, non-Newtonian fluid, wall transpiration.

1 Introduction

Convection heat transfer from vertical surfaces and wedges embedded in porous media has been the subject of many investigations. This is due to the fact that these flows have many engineering and geophysical applications such as geothermal reservoirs, drying of porous solids, thermal insulation, enhanced oil recovery, groundwater pollution, and underground energy transport. Cheng and Minkowycz [1] have presented similarity solutions for free thermal convection from a vertical plate in a fluid-saturated porous medium. Ranganathan and Viskanta [2] have considered mixed convection boundary layer flow along a vertical surface in a porous medium. Nakayama and Koyama [3] have suggested similarity transformations for pure, combined and forced convection in Darcian and non-Darcian porous media. Lai [4] has investigated coupled heat and mass transfer by mixed convection from an isothermal vertical plate in a porous medium. Hsieh et al. [5] have presented non-similar solutions for combined convection in porous media. Yih [6] has studied the effect of uniform suction/blowing on heat transfer of MHD Hiemenz flow through porous media. Kumari et al. [7] have studied mixed convection flow over a vertical wedge embedded in highly porous medium. Yih [8] has reported on the radiation effects on the entire regime of mixed convection over an isothermal wedge in the porous media. Also, Yih [9] has studied coupled heat and mass transfer in mixed convection over a wedge with variable wall temperature and concentration in porous media. All of the above references considered Newtonian fluids.

A number of industrially important fluids such as molten plastics, polymers, pulps, foods and slurries and fossil fuels which may saturate underground beds display non-Newtonian fluid behavior. Non-Newtonian fluids exhibit a non-linear relationship between shear stress and shear rate. Chen and Chen [10] have presented similarity solutions for free convection of non-Newtonian fluids over vertical surfaces in porous media. Mehta and Rao [11] have investigated buoyancy-induced flow of non-Newtonian fluids over a non-isothermal horizontal plate embedded in a porous medium. Also, Mehta and Rao [12] have analyzed buoyancy-induced flow of non-Newtonian fluids in a porous medium past a vertical plate with non-uniform surface heat flux. In a series of papers, Gorla and co-workers [13-18] have studied mixed convection in non-Newtonian fluids along horizontal and vertical plates in porous media. Also, Mansour and Gorla [19] have studied mixed convection–radiation interaction in power-law fluids along a non-isothermal wedge embedded in a porous medium. Jumah and Mujumdar [20] have considered free convection heat and mass transfer of non-Newtonian power-law fluids with yield stress from a vertical flat plate in saturated porous

media. Recently, Chamkha and Al-Humoud [21] studied mixed convection heat and mass transfer of non-Newtonian fluids from a permeable surface embedded in a porous medium under uniform surface temperature and concentration species.

In certain porous media applications such as those involving heat removal from nuclear fuel debris, underground disposal of radioactive waste material, storage of food stuffs, and exothermic chemical reactions and dissociating fluids in packed-bed reactors, the working fluid heat generation or absorption effects are important. A simulation of such situations requires the addition of a heat source or sink term in the energy equation. This term has been assumed to be either a constant (Acharya and Goldstein [22] or temperature-dependent (Vajravelu and Nayfeh [23]).

The effects of fluid wall suction or injection the flow and heat transfer characteristics along vertical semi-infinite plates have been investigated by several authors (Cheng [24], Lai and Kulacki [25,26], Minkowycz et al. [27] and Hooper et al. [28]). Some of these studies have reported similarity solutions (Cheng [24] and Lai and Kulacki [25,26]) while others have obtained non-similar solutions (Minkowycz, et al. [27] and Hooper et al. [25]). Lai and Kulacki [25,26] have reported similarity solutions for mixed convection flow over horizontal and inclined plates embedded in fluid-saturated porous media in the presence of surface mass flux. On the other hand, Minkowycz et al. [27] have discussed the effect of surface mass transfer on buoyancy-induced Darcian flow adjacent to a horizontal surface using non-similarity solutions. Also, Hooper et al. [28] have considered the problem of non-similar mixed convection flow along an isothermal vertical plate in porous media with uniform surface suction or injection and introduced a single parameter for the entire regime of free-forced-mixed convection. Their non-similar variable represented the effect of suction or injection at the wall.

The objective of this paper is to consider coupled heat and mass transfer by mixed convection for a non-Newtonian power-law fluid flow over a permeable wedge embedded in a fluid-saturated porous medium under variable wall temperature and concentration and in the presence of wall transpiration and heat generation or absorption effects.

2 Problem Formulation

Consider steady heat and mass transfer by mixed convective flow of a non-Newtonian power-law fluid over a wedge embedded in a porous medium with variable temperature and concentration. The power-law model of Ostwald-de-Waele which is adequate for many non-Newtonian fluids is considered in the present work. The porous medium is assumed to be uniform, isotropic and in local thermal equilibrium with the fluid. All fluid properties are assumed to be constant. Under the Boussinesq and boundary-layer approximations, the governing equations for this problem can be written as

$$\frac{\partial u}{\partial x}+\frac{\partial v}{\partial y}=0 \tag{1}$$

$$nu^{n-1}\frac{\partial u}{\partial y}=\frac{K}{\mu}\rho g\left[\beta_T\frac{\partial T}{\partial y}+\beta_c\frac{\partial c}{\partial y}\right] \tag{2}$$

$$u\frac{\partial T}{\partial x}+v\frac{\partial T}{\partial y}=\alpha_e\frac{\partial^2 T}{\partial y^2}+\frac{Q_o}{\rho c_p}(T-T_\infty) \tag{3}$$

$$u\frac{\partial c}{\partial x}+v\frac{\partial c}{\partial y}=D\frac{\partial^2 c}{\partial y^2} \tag{4}$$

where x and y denote the vertical and horizontal directions, respectively. u, v, T and c are the x- and y-components of velocity, temperature and concentration, respectively. ρ, c_p, μ, n and D are the fluid density, specific heat at constant pressure, consistency index for viscosity, power-law fluid viscosity index, and mass diffusion coefficient, respectively. K and α_e are the porous medium modified permeability and effective thermal diffusivity, respectively. β_T, β_c, Q_o and T_∞ are the thermal expansion coefficient, concentration expansion coefficient, heat generation (>0) or absorption (<0) coefficient and the free stream temperature, respectively.

The modified permeability of the porous medium K for flows of non-Newtonian power-law fluids is given by:

$$K=\frac{1}{2C_t}\left(\frac{n\varepsilon}{3n+1}\right)^n\left(\frac{50k^*}{3\varepsilon}\right)^{(n+1)/2} \tag{5}$$

where

$$k^*=\frac{\varepsilon^3 d^2}{150(1-\varepsilon)^2} \tag{6}$$

$$C_t=\begin{cases}\dfrac{25}{12}, \text{ Christopher and Middleman[29]}\\ \dfrac{2}{3}\left(\dfrac{8n}{9n+3}\right)\left(\dfrac{10n-3}{6n+1}\right)\left(\dfrac{75}{16}\right)^{3(10n-3)/(10n+11)}\\ \text{Dharmadhikari and Kale[30]}\end{cases}, \tag{7}$$

where ε and d is the porosity and the particle diameter of the packed-bed porous medium.

The boundary conditions suggested by the physics of the problem are given by

$$v(x,0)=v_o, T_w(x)=T_\infty+ax^\lambda, c_w(x)=c_\infty+bx^\lambda$$
$$u(x,\infty)=U_\infty, T(x,\infty)=T_\infty, c(x,\infty)=c_\infty \quad (8)$$

where v_o, T_w and c_w are the wall transpiration constant, wall temperature and wall concentration, respectively. The parameters a, b and λ are constants and U_∞, T_∞ and c_∞ are the free stream velocity, temperature and concentration, respectively.

It is convenient to transform the governing equations into a non-similar dimensionless form which can be suitable for solution as an initial-value problem. This can be done by introducing the stream function such that

$$u=\frac{\partial\psi}{\partial y}, v=-\frac{\partial\psi}{\partial x} \quad (9)$$

and using

$$\eta=\frac{y}{x}\left(Pe_x^{1/2}\right)\chi^{-1} \quad (10a)$$

$$\psi=\alpha_e\left(Pe_x^{1/2}\right)\chi^{-1}f(\chi,\eta) \quad (10b)$$

$$\theta=\frac{T-T_\infty}{T_w-T_\infty} \quad (10c)$$

$$C=\frac{c-c_\infty}{c_w-c_\infty} \quad (10d)$$

$$U_\infty=c^*x^m, m=\frac{\delta}{2\pi-\delta} \quad (10e)$$

where $Pe_x=U_\infty x/\alpha_e$ and $Ra_x=(x/\alpha_e)[\rho g\beta_T(T_w-T_\infty)\,K/(\mu)]^{1/n}$ are the local Peclet and modified Rayleigh numbers, respectively. The parameters c^* and δ are a free stream velocity constant and the half-wedge angle, respectively.

Substituting Eqs. (9) and (10) into Eqs. (1) through (4) produces the following non-similar equations:

$$nf'^{n-1}f''=(1-\chi)^{2n}(\theta'+NC') \quad (11)$$

$$\theta''+\frac{1}{2}\left[(m+1)+\left(\frac{\lambda-mn}{n}\right)(1-\chi)\right]f\theta'-\lambda f'\theta+\phi\theta = -\left(\frac{\lambda-mn}{2n}\right)\chi(1-\chi)\left(f'\frac{\partial\theta}{\partial\chi}-\theta'\frac{\partial f}{\partial\chi}\right) \quad (12)$$

$$\frac{1}{Le}C''+\frac{1}{2}\left[(m+1)+\left(\frac{\lambda-mn}{n}\right)(1-\chi)\right]fC'-\lambda f'C = -\left(\frac{\lambda-mn}{2n}\right)\chi(1-\chi)\left(f'\frac{\partial C}{\partial\chi}-C'\frac{\partial f}{\partial\chi}\right) \quad (13)$$

$$\frac{1}{2}\left[(m+1)+\left(\frac{\lambda-mn}{n}\right)(1-\chi)\right]f(\chi,0)+\left(\frac{\lambda-mn}{2n}\right)\chi(1-\chi)\frac{\partial f}{\partial\chi}(\chi,0)=f_o, \theta(\chi,0)=1, C(\chi,0)=1$$
$$f'(\chi,\infty)=\chi^2,\ \theta(\chi,\infty)=0,\ C(\chi,\infty)=0 \quad (14)$$

where

$$Le=\frac{\alpha_e}{D},\ N=\frac{\beta_c b}{\beta_T a},\ \chi=\left[1+\left(\frac{Ra_x}{Pe_x}\right)^{1/2}\right]^{-1},$$
$$\phi=\frac{Q_o x^2\chi^2}{\rho c_p\alpha_e Pe_x}, f_o=\frac{v_o x\chi}{\alpha_e Pe_x^{1/2}} \quad (15)$$

are the Lewis number, concentration to thermal buoyancy ratio, mixed convection parameter, heat generation or absorption parameter and the dimensionless wall transpiration parameter, respectively. It should be noted that $\chi = 0$ ($Pe_x = 0$) corresponds to pure free convection while $\chi = 1$ ($Ra_x = 0$) corresponds to pure forced convection. The entire regime of mixed convection corresponds to values of χ between 0 and 1.

Of special significance for this problem are the local Nusselt and Sherwood numbers. These physical quantities can be defined as

$$Nu_x=-(Pe_x)^{1/2}\chi^{-1}\theta'(\chi,0); \quad (17)$$
$$Sh_x=-(Pe_x)^{1/2}\chi^{-1}C'(\chi,0); \quad (18)$$

3 Numerical Method and Validation

Equations (11) through (14) represent an initial-value problem with χ playing the role of time. This general non-linear problem can not be solved in closed form and, therefore, a numerical solution is necessary to describe the physics of the problem. The implicit, tri-diagonal finite-difference method similar to that discussed by Blottner [31] has proven to be adequate and sufficiently accurate for the solution of this kind of problems. Therefore, it is adopted in the present work.

All first-order derivatives with respect to χ are replaced by two-point backward-difference formulae when marching in the positive χ direction and by two-point forward-difference formulae when marching in the negative ξ direction. Then, all second-order differential equations in η are discretized using three-point central difference quotients. This discretization process produces a tri-diagonal set of algebraic equations at each line of constant χ which is readily solved by the well known Thomas algorithm (see Blottner [31]). During the solution, iteration is employed to deal with the non-linearity aspect of the governing differential equations. The problem is solved line by line starting with line χ=0 where similarity equations are solved to obtain the initial profiles of velocity, temperature and concentration and marching forward (or backward) in χ until the desired line of constant χ is reached. Variable step sizes in the η direction with $\Delta\eta_1 = 0.001$ and a growth factor G = 1.04 such that $\Delta\eta_n = G\Delta\eta_{n-1}$ and constant step sizes in the χ direction with $\Delta\chi = 0.01$ are employed. These step sizes are arrived at after many numerical

experimentations performed to assess grid independence. The convergence criterion employed in the present work is based on the difference between the current and the previous iterations. When this difference reached 10^{-5} for all points in the η directions, the solution was assumed converged and the iteration process was terminated.

Tables 1 and 2 present a comparison of $-\theta'(\chi,0)$ and $-C'(\chi,0)$ at selected values of m and χ between the results of the present work and those reported earlier by Yih [9] for a Newtonian fluid (n=1) with Le=1, N=1 and λ=0. It is clear from this comparison that a good agreement between the results exists. This lends confidence in the correctness of the numerical results to be reported subsequently.

Table 1. Values of $-\theta'(\chi,0)$ and $-C'(\chi,0)$ at selected values of m and χ for f_o=0, Le=1, n=1, N=1, λ=0 and ϕ=0. (Present work)

	$-\theta'(\chi,0)$		$-C'(\chi,0)$	
	m=0	m=1	m=0	m=1
χ=0.0	0.62781	0.62781	0.62781	0.62781
χ=0.2	0.51498	0.52011	0.51498	0.52011
χ=0.5	0.42381	0.47351	0.42381	0.47351
χ=0.8	0.46879	0.63913	0.46879	0.63913
χ=1.0	0.56410	0.79806	0.56410	0.79806

Table 2. Values of $-\theta'(\chi,0)$ and $-C'(\chi,0)$ at selected values of m and χ for f_o=0, Le=1, n=1, N=1, λ=0 and ϕ=0. (Yih [9])

	$-\theta'(\chi,0)$		$-C'(\chi,0)$	
	m=0	m=1	m=0	m=1
χ=0.0	0.6276	0.6276	0.6276	0.6276
χ=0.2	0.5151	0.5189	0.5151	0.5189
χ=0.5	0.4238	0.4703	0.4238	0.4703
χ=0.8	0.4689	0.6395	0.4689	0.6395
χ=1.0	0.5642	0.7979	0.5642	0.7979

4 Results and Discussion

In this section, a representative set of numerical results is presented graphically in Figs. 1-20 to illustrate special features of the solution.

Figures 1 and 2 present typical temperature and concentration profiles for various values of the buoyancy ratio N and the power-law fluid viscosity index n, respectively. In general, increases in the value of N have the tendency to cause more induced flow along the wedge surface. This behavior in the flow velocity is accompanied by decreases in the fluid temperature and concentration species as well as decreases in the thermal and concentration boundary layers as N increases from -1 to 5. On the other hand, as the power-law fluid viscosity index n increases, the fluid temperature and solute concentration as well as their boundary layers increase as clearly seen from Figs. 1 and 2.

Figures 3 and 4 illustrate the influence of the buoyancy ratio N in the entire range of the mixed convection parameter $0 \leq \chi \leq 1$ on the reduced local Nusselt number $[\,Nu = -\theta'(\chi,0)\,]$ and the reduced local Sherwood number $[\,Sh = -C'(\chi,0)\,]$ for power-law fluid viscosity indices n=0.7 (shear-thinning or pseudo-plastic fluid), n=1.0 (Newtonian fluid) and n=1.5 (shear-thickening or dilatant fluid), respectively. The decreases in the luid temperature and solute concentration as N increases mentioned above causes the negative values of the wall temperature and concentration slopes to increase yielding increases in both the local Nusselt and Sherwood numbers in the entire range of mixed convection parameter $0 \leq \chi < 1$. However, for χ=1 (forced convection limit), the flow is uncoupled from the thermal and solutal buoyancy effects and therefore, the local Nusselt and Sherwood numbers are constant for all values of N. This is true for all values of the power-law fluid index n. From the definition of χ, it is seen that increases in the value of the parameter Ra_x/Pe_x causes the mixed convection parameter χ to decrease. Thus, small values of Ra_x/Pe_x correspond to values of χ close to unity which indicate almost pure forced convection regime. On the other hand, high values of Ra_x/Pe_x correspond to values of χ close to zero which indicate almost pure free convection regime. Furthermore, moderate values of Ra_x/Pe_x represent values of χ between 0 and 1 which correspond to the mixed convection regime. For the forced convection limit (χ = 1) it is clear from Eq. (11) that the velocity in the boundary layer f' is uniform irregardless of the value of n. However, for smaller values of χ (higher values of Ra_x/Pe_x) at a fixed value of N and n=1.0, the buoyancy effect increases. As this occurs, the fluid velocity close to the wall increases for values of $\chi \leq 0.5$ due to the buoyancy effect which becomes maximum for χ = 0 (free convection limit). This decrease and increase in the fluid velocity f' as χ is decreased from unity to zero is accompanied by a respective increase and a decrease in

the fluid temperature and concentration. As a result, the local Nusselt and Sherwood numbers tend to decrease and then increase as χ is increased from 0 to unity forming slight dips. The location of these dips depends on the value of n and N as seen from Figs. 3 and 4.

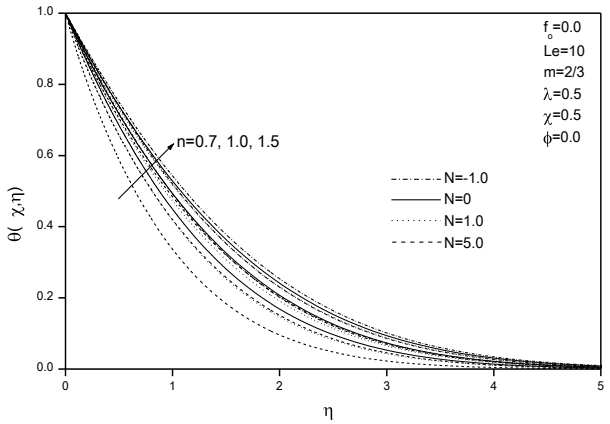

Fig. 1. Effects of n and N on temperature profiles

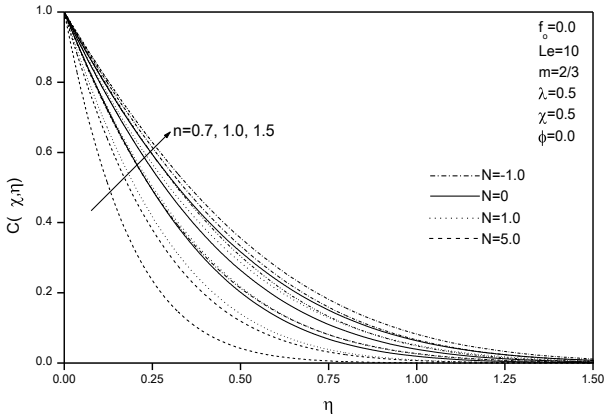

Fig. 2. Effects of n and N on concentration profiles

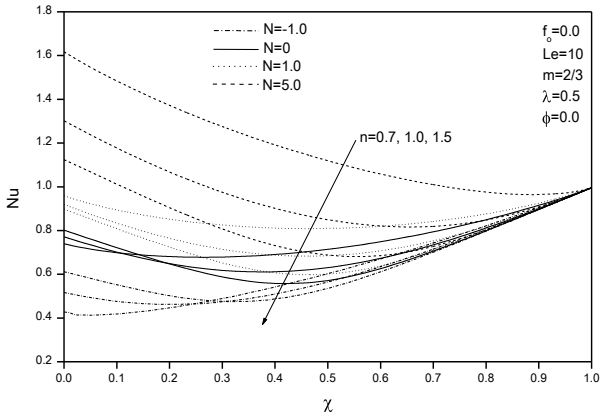

Fig. 3. Effects of n and N on local Nusselt number for different χ values

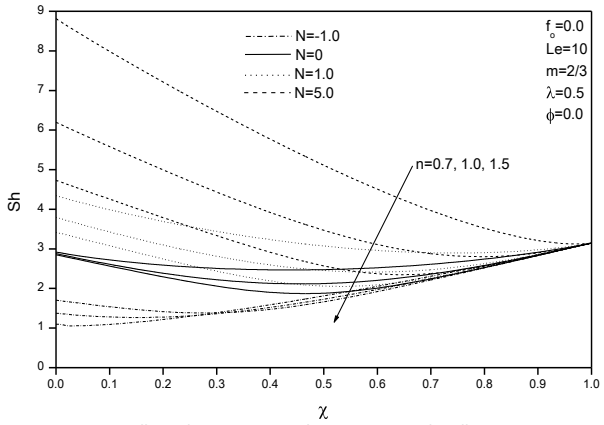

Fig. 4. Effects of n and N on local Sherwood number for different χ values

Also, it is clearly observed from Figs. 3 and 4 that, in general, the local Nusselt and Sherwood numbers decrease as the power-law fluid index n increases. However, this is not true for all values of χ depending on the value of the buoyancy ratio N. It is predicted that for N>0, the value of Nu and Sh decrease as n increases in the entire range $0 \leq \chi < 1$. However, for $N \leq 0$ the values of Nu and Sh increase as n increases for small values of χ (for example $\chi<0.3$ for N=-1) while the local Nusselt and Sherwood numbers decrease with increasing values of n in the rest of the range (for example $0.3 \leq \chi < 1$ for N=-1). All these features are clear from Figs. 3 and 4.

Figures 5 and 6 show representative temperature and concentration profiles for different values of the wall temperature or concentration index λ and power-law fluid index n, respectively. It is clearly observed that both the fluid temperature and solute concentration decrease while the negative values of their wall slopes increase as λ increases. This yields enhancements in both heat and mass transfer effects.

Figures 7 and 8 present the effects of the variable wall temperature (or concentration) index λ on the reduced local Nusselt number Nu and reduced local Sherwood number Sh for n=0.7, 1.0 and 1.5 in the entire range $0 \leq \chi \leq 1$, respectively. As mentioned before, increasing the wall temperature (or concentration) index λ causes enhancements in both the heat and mass transfer effects represented by increases in both the reduced local Nusselt and Sherwood numbers in the entire range $0 \leq \chi < 1$. As indicated before, since N=5 in these figures, it is seen that Nu and Sh decrease with increasing values of n in the entire range $0 \leq \chi < 1$.

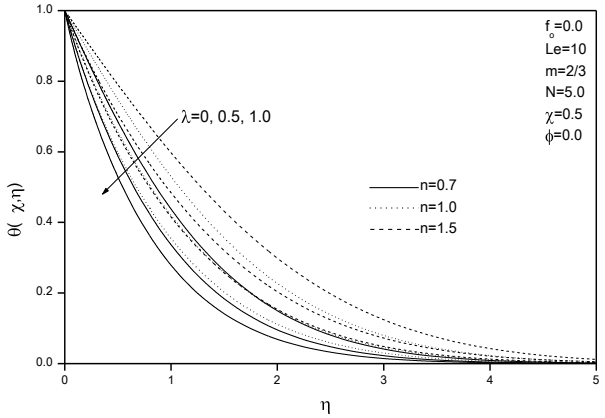

Fig. 5. Effects of n and λ on temperature profiles

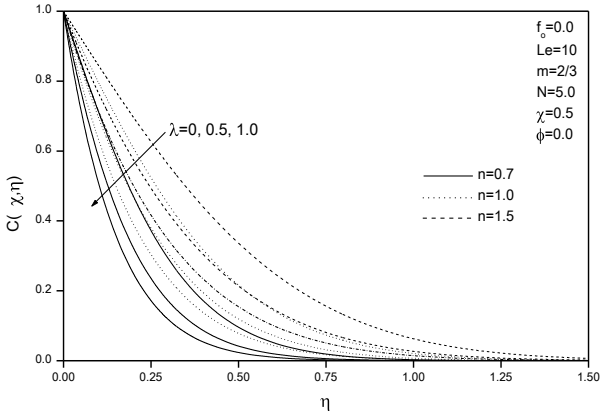

Fig. 6. Effects of n and λ on concentration profiles

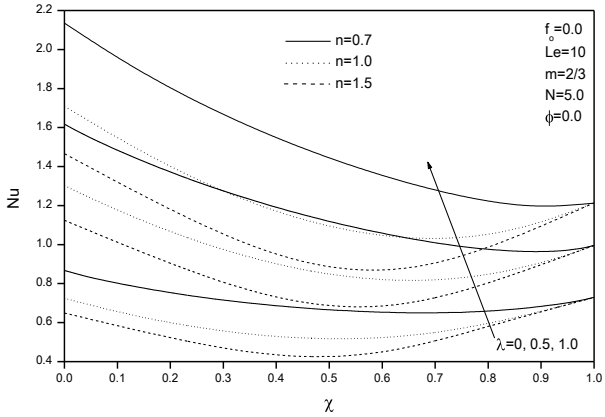

Fig. 7. Effects of n and λ on local Nusselt number for different χ values

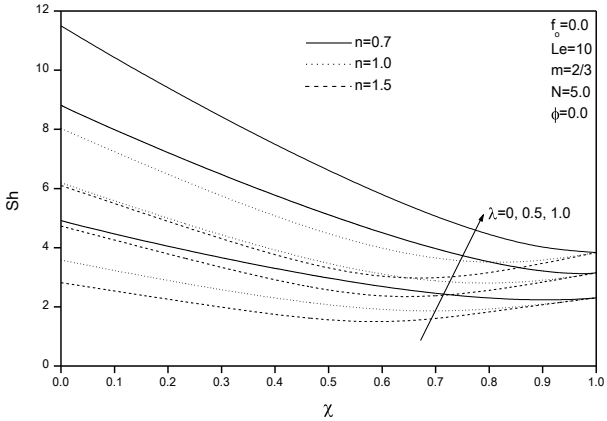

Fig. 8. Effects of n and λ on local Sherwood number for different χ values

Figures 9 and 10 show the effects of increasing the Lewis number on the temperature and concentration profiles for various values of n, respectively. As expected, the fluid temperature increases while the solute concentration and its boundary-layer thickness decrease considerable as the Lewis number Le increases.

Figures 11 and 12 depict the influence of the Lewis number Le on the values of Nu and Sh in the entire mixed convection range $0 \leq \chi \leq 1$ for different values of n, respectively. Increasing the value of the Lewis number results in decreasing the concentration profile and increasing the temperature profile causing the values of Sh and Nu to increase and decrease, respectively as Le increases.

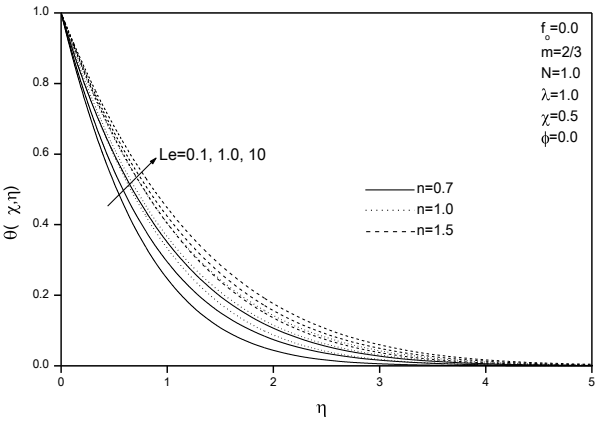

Fig. 9. Effects of n and Le on temperature profiles

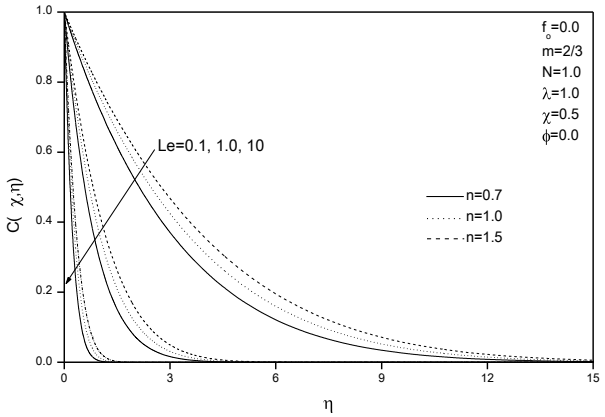

Fig. 10. Effects of n and Le on concentration profiles

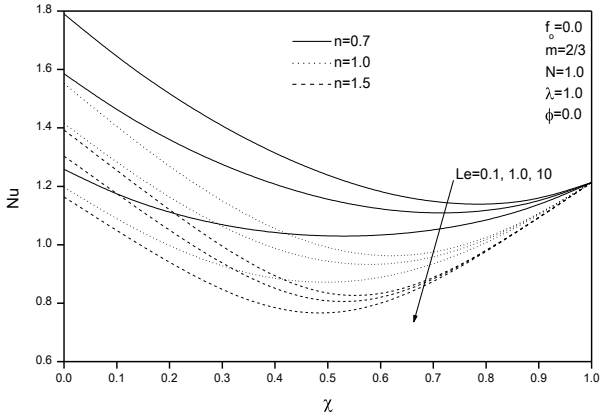

Fig. 11. Effects of n and Le on local Nusselt number for different χ values

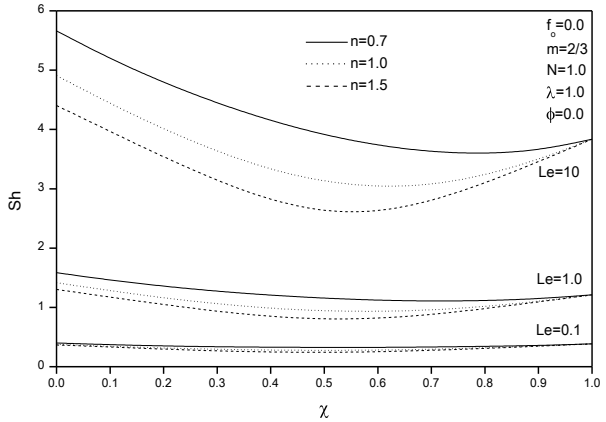

Fig. 12. Effects of n and Le on local Sherwood number for different χ values

In Figs. 13 and 14, the effects of the free stream velocity exponent m on the temperature and concentration profiles are respectively shown. It is predicted that as the value of m increases, both the fluid temperature and solute concentration decrease with slight effect of their boundary-layer thicknesses.

Figures 15 and 16 illustrate the effects of the free stream velocity exponent m on the values of the reduced local Nusselt and Sherwood numbers (Nu and Sh) for n=0.7, 1 and 1.5 in the range $0 \leq \chi \leq 1$, respectively. It is clearly observed from these figures that the values of both Nu and Sh increase as the value of m increases. This is true for all values of n and in the entire range $0 \leq \chi \leq 1$. However, the effect of m is very small for small values of χ and becomes more pronounced as χ increases reaching its maximum at χ=1.

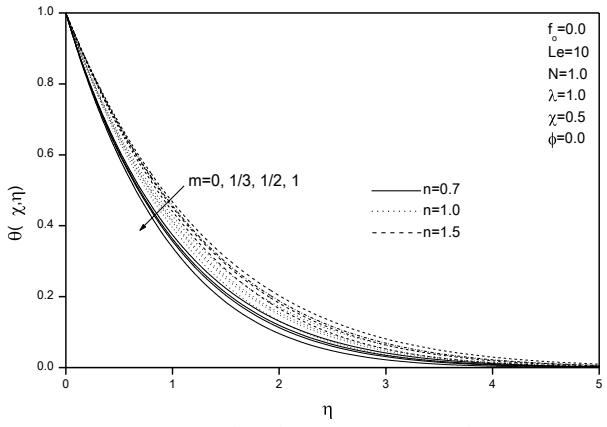

Fig. 13. Effects of n and m on temperature profiles

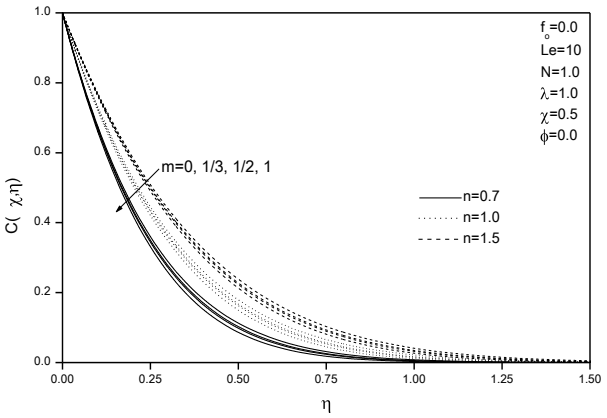

Fig. 14. Effects of n and m on concentration profiles

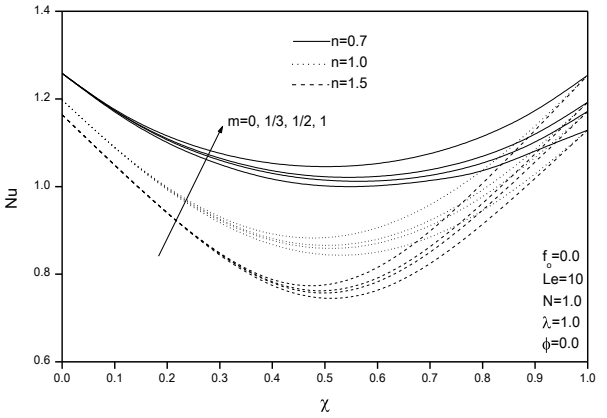

Fig. 15. Effects of n and m on local Nusselt number for different χ values

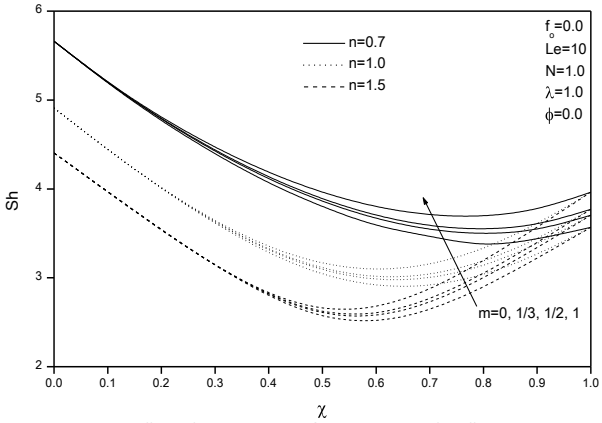

Fig. 16. Effects of n and m on local Sherwood number for different χ values

Figures 17 and 18 display typical temperature and concentration profiles for various values of the transpiration and heat generation or absorption parameters (f_o and ϕ), respectively. Increases in the transpiration parameter f_o have the tendency to decrease both the fluid temperature and solute concentration. On the other hand, increasing the heat generation or absorption parameter ϕ causes increases in the fluid temperature with insignificant effect on the distribution of the concentration species. These behaviors are clearly shown in Figs. 17 and 18.

Finally, Figs. 19 and 20 depict the effects of the transpiration parameter f_o and the heat generation or absorption parameter ϕ on the reduced local Nusselt and Sherwood numbers (Nu and Sh) in the entire range $0 \leq \chi \leq 1$, respectively. It is observed that the reduced local Nusselt and Sherwood numbers increase as the transpiration parameter increases where as the reduced local Nusselt number decreases and the reduced local Sherwood number remains almost unchanged as the heat generation or absorption parameter increases in the entire range $0 \leq \chi \leq 1$.

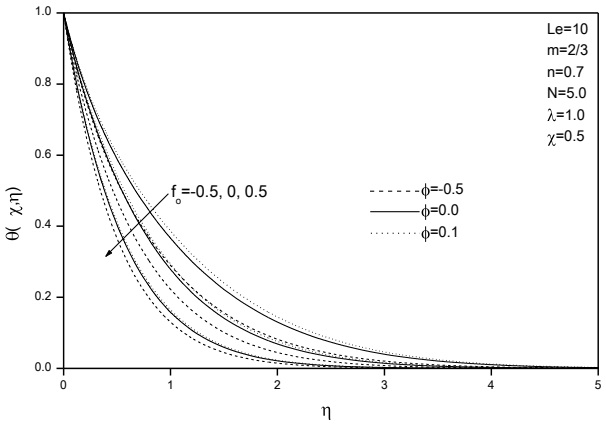

Fig. 17. Effects of f_o and ϕ on temperature profiles

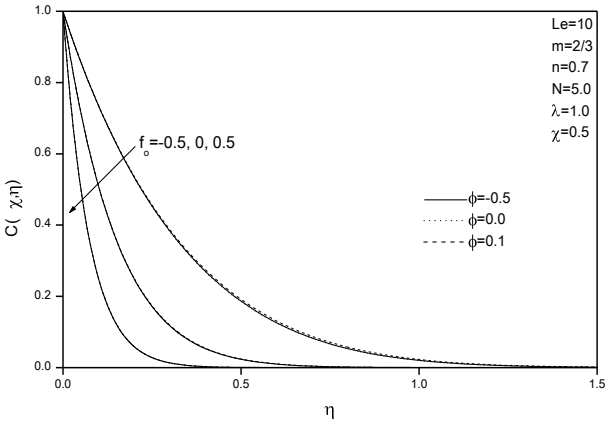

Fig. 18. Effects of f_0 and ϕ on concentration profiles

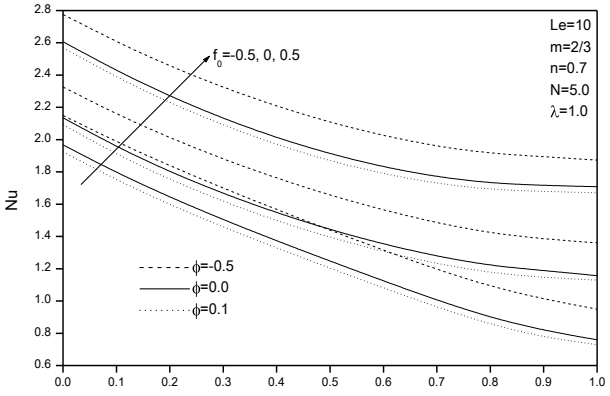

Fig. 19. Effects of f_o and ϕ on local Nusselt number for different χ values

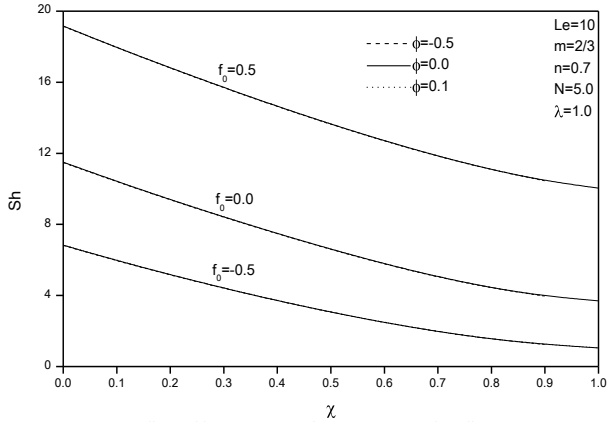

Fig. 20. Effects of f_0 and ϕ on local Sherwood number for different χ values

5 Conclusion

This work considered coupled heat and mass transfer by mixed convective flow of a non-Newtonian power-law fluid along a permeable wedge embedded in a porous medium under variable wall temperature and

concentration in the presence of heat generation or absorption effects. A single parameter for the entire range of free-forced-mixed convection regime was employed. The obtained non-similar differential equations were solved numerically by an efficient implicit finite-difference method. The results focused on the effects of the buoyancy ratio, power-law fluid index, mixed convection parameter, wall temperature or concentration, Lewis number, free stream velocity exponent, transpiration parameter and the heat generation or absorption parameter on the reduced local Nusselt and Sherwood numbers. It was found that as the buoyancy ratio was increased, both the reduced local Nusselt and Sherwood numbers increased in the entire range of free and mixed convection regime while they remained constant for the forced-convection regime for all power-law fluid index values. However, they decreased and then increased forming dips as the mixed-convection parameter was increased from the free-convection limit to the forced-convection limit. Also, the reduced local Nusselt and Sherwood numbers increased with increasing values of the wall temperature or concentration index. In addition, it was concluded that in general, the reduced local Nusselt and Sherwood numbers decreased as the power-law fluid index was increased. Increasing the Lewis number produced increases in the reduced local Sherwood number and decreases in the reduced local Nusselt number. Furthermore, both of the reduced local Nusselt and Sherwood numbers increased as the free stream velocity exponent increased. Moreover, the reduced local Nusselt and Sherwood numbers increased as the transpiration parameter increased where as the reduced local Nusselt number decreased and the reduced local Sherwood number remained almost unchanged as the heat generation or absorption parameter increased.

Acknowledgement: The author acknowledges and thanks the financial support of PAAET research administration through Project TS-09-08.

References:

1. P. Cheng and W.J. Minkowycz, Free convection about a vertical flat plate embedded in a porous medium with application to heat transfer from a dike," *J. of Geophys. Res.*, Vol. 82, 1977, pp. 2040-2044.
2. P. Ranganathan and R. Viskanta, Mixed convection boundary layer flow along a vertical surface in a porous medium, *Numerical Heat Transfer*, Vol. 7, 1984, pp. 305-317.
3. A. Nakayama and H.A. Koyama, General similarity transformation for free, forced and mixed convection in Darcy and non-Darcy porous media, *J. Heat Transfer*, Vol. 109, 1987, pp. 1041-1045.
4. F.C. Lai, Coupled heat and mass transfer by mixed convection from a vertical plate in a saturated porous medium, *Int. Commun. Heat Mass Transfer*, Vol. 18, 1991, pp. 93-106.
5. J.C. Hsieh, T.S. Chen and B.F. Armaly, Non-similarity solutions for mixed convection from vertical surfaces in a porous medium, *Int. J. Heat Mass Transfer*, Vol. 36, 1993, pp. 1485-1493.
6. K.A. Yih, The effect of uniform suction/blowing on heat transfer of magnetohydrodynamic Hiemenz flow through porous media, *Acta Mech.*, Vol. 130, 1998, pp. 147-158.
7. M. Kumari, H.S. Takhar and G. Nath, Mixed convection flow over a vertical wedge embedded in highly porous medium, *Heat and Mass Transfer*, Vol. 37, 2001, pp. 139-146.
8. K.A. Yih, Radiation effects on mixed convection over an isothermal wedge in the porous media: The entire regime. *Heat Transfer Engineering*, Vol. 22, 2001, pp. 26-32.
9. K.A. Yih, Coupled heat and mass transfer in mixed convection over a wedge with variable wall temperature and concentration in porous media: The entire regime, *Int. Commun. Heat Mass Transfer*, Vol. 25, 1998, pp. 1145-1158.
10. H.T. Chen and C.K. Chen, Free convection of non-Newtonian fluids along a vertical plate embedded in a porous medium, *Trans. ASME, J. Heat Transfer*, Vol. 110, 1988, pp. 257-260.
11. K.N. Mehta and K.N. Rao, Buoyancy-induced flow of non-Newtonian fluids over a non-isothermal horizontal plate embedded in a porous medium, *Int. J. Eng. Sci.*, Vol. 32, 1994, pp. 521–525.
12. K.N. Mehta and K.N. Rao, Buoyancy-induced flow of non-Newtonian fluids in a porous medium past a vertical plate with nonuniform surface heat flux, *Int. J. Eng. Sci.*, Vol. 32, 1994, pp. 297–302.
13. R.S.R. Gorla, A. Slaouti and H.S. Takhar, Mixed convection in non-Newtonian fluids along a vertical plate in porous media with surface mass transfer, *International Journal of Numerical Methods for Heat & Fluid Flow*, Vol. 7, 1997, pp. 598-608.
14. M. Kumari, R.S.R. Gorla and L. Byrd, Mixed convection in non-Newtonian fluids along a horizontal plate in a porous medium, *Trans. ASME, J. Energy Resour. Technol.*, Vol. 119, 1997, pp. 34-37.
15. R.S.R. Gorla, K. Shanmugam and M. Kumari, Nonsimilar solutions for mixed convection in non-Newtonian fluids along horizontal surfaces in porous media, *Transport in Porous Media*, Vol. 28, 1997, pp. 319-334.

16. R.S.R. Gorla, K. Shanmugam and M. Kumari, Mixed convection in non-Newtonian fluids along nonisothermal horizontal surfaces in porous media, *Heat and Mass Transfer*, Vol. 33, 1998, pp. 281-286.
17. R.S.R. Gorla and M. Kumari, Nonsimilar solutions for mixed convection in non-Newtonian fluids along a vertical plate in a porous medium, *Transport in Porous Media*, Vol. 33, 1998, pp. 295–307.
18. R.S.R. Gorla and M. Kumari, Mixed convection in non-Newtonian fluids along a vertical plate with variable surface heat flux in a porous medium, *Heat and Mass Transfer*, Vol. 35, 1999, pp. 221–227.
19. M.A. Mansour and R.S.R. Gorla, Mixed convection–radiation interaction in power-law fluids along a nonisothermal wedge embedded in a porous medium, *Transport in Porous Media*, Vol. 30, 1998, pp. 113-124.
20. R.Y. Jumah and A.S. Mujumdar, Free convection heat and mass transfer of non-Newtonian power law fluids with yield stress from a vertical flat plate in saturated porous media, *Int. Commun. Heat Mass Transfer*, Vol. 27, 2000, pp. 485-494.
21. A.J. Chamkha and J. Al-Humoud, Mixed convection heat and mass transfer of non-Newtonian fluids from a permeable surface embedded in a porous medium, *Int. J. Numer. Meth. Heat & Fluid Flow*, Vol. 17, 2007, pp. 195-212.
22. S. Acharya and R.J. Goldstein, Natural convection in an externally heated vertical or inclined box containing internal energy sources, *J. Heat Transfer*, Vol. 107, 1985, pp. 855-866.
23. K. Vajravelu and J. Nayfeh, Hydromagnetic convection at a cone and a wedge, *Int. Commun. Heat Mass Transfer*, Vol. 19, 1992, pp. 701-710.
24. P. Cheng, The influence of lateral mass flux on free convection boundary layers in a saturated porous medium, *Int. J. Heat Mass Transfer*, Vol. 20, 1977, pp. 201-206.
25. F.C. Lai and F.A. Kulacki, The influence of surface mass flux on mixed convection over horizontal plates in saturated porous media, *Int. J. Heat Mass Transfer*, Vol. 33, 1990, pp. 576-579.
26. F.C. Lai and F.A. Kulacki, The influence of lateral mass flux on mixed convection over inclined surfaces in saturated porous media, *J. Heat Transfer*, Vol. 112, 1990, pp. 515-518.
27. W.J. Minkowycz, P. Cheng and F. Moalem, The effect of surface mass transfer on buoyancy-induced Darcian flow adjacent to a horizontal heated surface, *Int. Commun. Heat Mass Transfer*, Vol. 12, 1985, pp. 55-65.
28. W.B. Hooper, T.S. Chen and B.F. Armaly, Mixed convection from a vertical plate in porous media with surface injection or suction, *Numer. Heat Transfer*, Vol. 25, 1993, pp. 317-329.
29. R.H. Christopher and S. Middleman, Power-law flow through a packed tube, *I & EC Fundamentals*, Vol. 4, 1965, pp. 422-426.
30. R.V. Dharmadhikari and D.D. Kale, Flow of non-Newtonian fluids through porous media, *Chemical Eng. Sci.*, Vol. 40, 1985, pp. 527-529.
31. F.G. Blottner, Finite-difference methods of solution of the boundary-layer equations, *AIAA Journal*, Vol. 8, 1970, pp. 193-205.